

## ORIGINAL ARTICLE

# Localized impacts and economic implications from high temperature disruption days under climate change

Tim Summers<sup>1</sup>  | Erik Mackie<sup>2,3</sup> | Risa Ueno<sup>3,4</sup> | Charles Simpson<sup>3,5</sup> |  
J. Scott Hosking<sup>3,6</sup> | Tudor Suci<sup>7</sup> | Andrew Coburn<sup>1</sup> | Emily Shuckburgh<sup>2,7</sup>

<sup>1</sup>Centre for Risk Studies, Judge Business School, University of Cambridge, Cambridge, UK

<sup>2</sup>Cambridge Zero, University of Cambridge, Cambridge, UK

<sup>3</sup>British Antarctic Survey, NERC, Cambridge, UK

<sup>4</sup>Department of Chemistry, University of Cambridge, Cambridge, UK

<sup>5</sup>Institute for Environmental Design and Engineering, University College London

<sup>6</sup>The Alan Turing Institute, London, UK

<sup>7</sup>Department of Computer Science & Technology, University of Cambridge, Cambridge, UK

## Correspondence

Tim Summers, Centre for Risk Studies, Cambridge Judge Business School, University of Cambridge, Trumpington Street, Cambridge CB2 1AG, UK.  
Email: [t.summers@jbs.com.ac.uk](mailto:t.summers@jbs.com.ac.uk)

## Abstract

Most studies into the effects of climate change have headline results in the form of a global change in mean temperature. More useful for businesses and governments, however, are measures of the localized impact, and also of extremes rather than averages. We have addressed this by examining the change in frequency of exceeding a daily mean temperature threshold, defined as ‘disruption days’, as it is often this exceedance which has the most dramatic impacts on personal or economic behaviour. Our exceedance analysis tackles the resolution of climate change both geographically and temporally, the latter specifically to address the 5- to 20-year time horizon which can be recognized in business planning.

We apply bias correction with quantile mapping to meteorological reanalysis data from ECMWF ERA5 and output from CMIP5 climate model simulations. By determining the daily frequency at which a mean temperature threshold is exceeded in this bias-corrected dataset, we can compare predicted and historic frequencies to estimate the change in the number of disruption days. Furthermore, by combining results from 18 different climate models, we can estimate the likelihood of more extreme events, taking into account model variations. This is useful for worst-case scenario planning.

Taking the city of Chicago as an example, the expected frequency of years with 40 or more disruption days above the 25°C threshold rises by a factor of four for a time period centred on 2040, compared with a period centred on 2000. Alternately, looking at the change in the number of days at a given likelihood, an example is Shenzhen, where the number of disruption days in a once-per-decade event exceeding the 25°C or 30°C threshold is expected to rise by a factor of four. In a future stage, superimposing these results onto maps of, for instance, GDP sensitivity or production days lost, will provide more accurate and targeted conclusions for future impacts of climate change. This method of quantifying costs on business-relevant timescales will enable businesses and governments

This is an open access article under the terms of the [Creative Commons Attribution](https://creativecommons.org/licenses/by/4.0/) License, which permits use, distribution and reproduction in any medium, provided the original work is properly cited.

© 2022 The Authors. *Climate Resilience and Sustainability* published by John Wiley & Sons Ltd on behalf of Royal Meteorological Society.

properly include risks associated with facilities, plan mitigating actions and make accurate provisions. It can also, for example, inform their disclosure of physical risks under the framework of the Task Force on Climate-related Financial Disclosures. This approach is equally applicable to other weather-related, localized phenomena likely to be impacted by climate change.

#### KEYWORDS

bias, climate, correction, disruption, economic, exceedance, temperature

## 1 | INTRODUCTION

Human-induced climate change has resulted in over 1.0°C of global warming to-date, when compared with pre-industrial levels (IPCC, 2021). The impacts of this warming trend on human and natural systems are already being felt around the world, in part through an increase in the likelihood of extreme weather events such as heatwaves (Ciavarella et al., 2021; Seneviratne et al., 2021). For example, the recent Siberian heatwave of summer 2020 has been shown to be at least 600 times more likely as a result of human-induced climate change (Ciavarella et al., 2021), while the probability of the conditions occurring that led to the 2019/2020 Australian bushfires is estimated to have increased by at least 30% since 1900, due to anthropogenic climate change (van Oldenborgh et al., 2020). These risks will increase with future warming.

The acute impact of climate change on business and society can be directly observed through changes to the tails of climatic distributions, as extreme events become more likely or more severe. But they are much harder to infer from apparently small changes in central statistics like the rise in the annual global average temperature. Extreme weather events can have adverse financial impacts on businesses through damage to physical assets, disruption or reduction in productivity of operations and supply chains, and impacts to market demand for products and services (Handmer et al., 2012).

These risks are of growing concern for businesses, and many corporations are trying to understand how present and future changes in extreme weather risk are likely to affect them. Organizations are under pressure to take action to address environmental, social and corporate governance demands, and for strategic and competitive reasons, as well as address regulatory requirements or other liabilities they may face. Mapping the geographical overlap of extreme weather events and business systems is key to providing insight to global corporates of the exposure of their entire value chains to physical climate change risk.

These needs are framed by the recommendations of the Task Force for Climate-related Financial Disclosures

(TCFD), which has been voluntarily adopted by more than 2,600 global organizations as of September 2021, and multiple nations around the world are now introducing legislation for official TCFD-aligned reporting requirements (Quarles, 2021). Investors are mobilizing to pressure companies to respond to the TCFD recommendations and disclose climate-related risks, with the threat that they will be less inclined to invest in companies that fail to do so (Eccles & Krzus, 2018). Companies that comply with the recommendations will have better strategies to adapt to climate change and may be more able to harness any potential opportunities that climate change presents.

The TCFD includes a recommendation to describe the impacts of acute (i.e. extreme) weather events, causing physical risks on an organization over three time horizons, typically below 5 years, 5–10 years and beyond 10 years. Organizations' energies are typically more focussed on short time-frames that they use to conduct operational, financial, strategic and capital planning (TCFD, 2020). However, the currently available data and model projections of future changes in extreme weather risk often do not suit the requirements of businesses. Organizations are struggling to reconcile the long-term projections of the consequences of a warmer planet in several decades' time with changes in the frequency, severity and geography of extreme weather events that are already having financial impacts on their businesses.

Economic productivity is particularly sensitive to extreme heat and associated hazards, which can affect large regions simultaneously to produce widespread impacts and economic loss (García-León et al., 2021; Handmer et al., 2012). These impacts are variable across sectors, and particularly affect those relying on labour-intensive activities such as agriculture, manufacturing and construction (Simpson et al., 2021; Zuo et al., 2015). Human output is impacted through time loss resulting from the heat-induced health outcomes, or 'absenteeism', as well as reductions in work productivity and capacity, termed 'presenteeism' (Xia et al., 2018). Infrastructure, transportation, and energy systems are also vulnerable to extreme heat, and physical damage or service outages

can severely disrupt supply chain activities and markets for products and services (Forzieri et al., 2018). Major cities, where economic activity is concentrated, are also subject to an urban heat island effect and so heatwaves are typically more extreme and can result in large death tolls and significant economic loss (Mora et al., 2017).

Here we present a geographic resolution of one arc degree grid squares as a starting point for risk assessment of global business activity, namely supply chains, transportation routes and retail distribution, and to demonstrate a methodology that can be refined and improved. This resolution corresponds to approximately a 110-km square at the equator, and a 110 km by 78 km rectangle at a temperate latitude of 45°.

## 2 | DATA AND METHODS

We use climate model outputs from the Coupled Model Intercomparison Project Phase 5 (CMIP5) to quantify future changes in extreme temperatures for the period 2020–2059, combined with recent historical data from the European Centre for Medium-Range Weather Forecasts (ECMWF) Re-Analysis (ERA5) for the period 1979–2018 (Hersbach et al., 2020, p. 5).<sup>1</sup> The metric used in this paper is the mean daily temperature. Although daily maximum or minimum temperatures, midday temperatures or other measures might be more appropriate for specific tasks (agricultural yields for instance often depend on minimum as well as maximum temperatures), the mean daily temperature is a good proxy for others and more representative of the overall risk, and thus a good starting point for this generalized study. A subset of 18 of the CMIP5 models is used: Details are given in the Appendix. For all models, only the RCP4.5 emissions scenarios are used as there is little divergence between the pathways prior to 2060. By the year 2040, the middle of the 2020–2059 period examined in this paper, the RCP4.5 scenario corresponds approximately to a 1.5°C warmer world, compared with pre-industrial temperatures. Information from the historical period is used to identify systematic biases between the climate model simulations and observational data at a local scale and this is used to produce a transfer function to bias-correct future projections.

A summary of the five-stage approach used is given below, followed by a more detailed description of each step:

1. ERA5 and CMIP5 data are first interpolated onto a common spatial grid.
2. For each of the models used, at each location, a bias correction to the raw data is calculated based on the observational data. This defines a transfer function that is then used on model predictions to bias-correct each model's future output.
3. Using the bias-corrected daily mean temperature predictions with specified temperature thresholds, the annual number of days that the mean daily temperature exceeds a defined threshold (the number of 'disruption days') is quantified.
4. The distribution of the number of disruption days is calculated over a 40-year period for each model at each location.
5. Combining outputs from all models gives an estimate of the likely number of disruption days, for a given temperature threshold, at each location for a specified time period.

### 2.1 | Re-gridding

ERA5 reanalysis and CMIP5 model outputs are interpolated onto a common spatial grid, a necessity given that different models use different grids. The grid is centred on squares one arc degree wide, between 70°S and 70°N, over landmass. This area is chosen since the majority of economic activity takes place over land mass away from the poles. For coastal locations, the centre of the cell used is the centroid of the land mass, to minimize the influence of the ocean. This results in data being obtained for approximately 18,000 geographic locations. While this resolution is high enough for many economic activities, any localized temperature influences (including topographic or urban heat island effect) may be under-represented.

### 2.2 | Bias correction

Statistical bias correction is a widely adopted post-processing procedure applied to climate model simulation outputs to produce location-specific future projections for impact modelling (e.g. Hawkins et al., 2013). This aims to remove the bias arising from model deficiencies and unresolved physical processes in an individual climate model. The application of bias correction is particularly important when aiming to capture extreme event features in climate model output, as is the focus of this study.

One assumption made with this bias-correcting method is that the biases are time-independent. It is possible that global climate systems show high non-linearities in biases,

<sup>1</sup> Data were accessed through the Centre for Environmental Data Analysis (CEDA), which makes the data available on JASMIN: <https://help.ceda.ac.uk/article/4465-cmip5-data>; Copernicus Climate Data Store, available from: <https://cds.climate.copernicus.eu/#!/search?text=ERA5&type=dataset>

for instance if a ‘tipping point’ is reached. We hope in the future to improve on the methods described here. Until then, these results should be taken as a best estimate. By including multiple independent models in the analysis, it is believed that this risk is mitigated to a degree. However, it is possible that future measurements could differ markedly from the results described in this paper through inherent uncertainty in our understanding of complex climate systems.

In this work, we adopt the quantile mapping method for bias correction, a popular distribution correction technique that has been found to outperform simpler bias correction methods that only account for the mean, or mean and variance of the climate variable (Gudmundsson et al., 2012). Quantile mapping is particularly effective in correcting the tails of a distribution, which is an important consideration in this work concerning extreme events.

It has been shown that applying quantile mapping to raw data can artificially alter the trends which can weaken the credibility of the resulting projection, and it has been argued that the climate change signal simulated by the model should be preserved (Haerter et al., 2011; Maraun, 2013). Therefore, we detrend the timeseries as a pre-processing step, and subsequently reintroduce the future model trend after applying quantile mapping. This encourages bias correction to account for daily variability without the long-term trend corrupting the overall distribution. We use a 31-day sliding window over the calendar year to avoid climatological discontinuity and use a linear regression to fit a trend for each window in order to capture the long-term signal that may depend on the time of year, as demonstrated by Hempel et al. (2013). A second-order polynomial is used to capture any acceleration in the future climate change signal, which was found to be more robust than a single linear fit (not shown). As with any statistical procedure, bias correction comes with a set of assumptions that are discussed extensively (e.g. Maraun & Widmann, 2018; Maraun et al., 2017).

The period 1979 to 2018 inclusive, comprising 40 years of daily data, for which we have overlapping ERA5 measurements and predictions from each CMIP5 model, is used to calibrate the bias-correcting transfer function. This is then applied to the future model simulations for the years 2020 to 2059 inclusive to obtain bias-corrected future projections. Transfer functions are derived for each model for every location, a total of approximately 330,000. Figure 1 illustrates an example for one location (Chicago) and one model (HadGEM2-CC): the summer daily mean temperature distribution of HadGEM2-CC output and corresponding ERA5 data, illustrating the discrepancy between them (top), and a timeseries of HadGEM2-CC, ERA5 and bias-corrected projection (bottom).

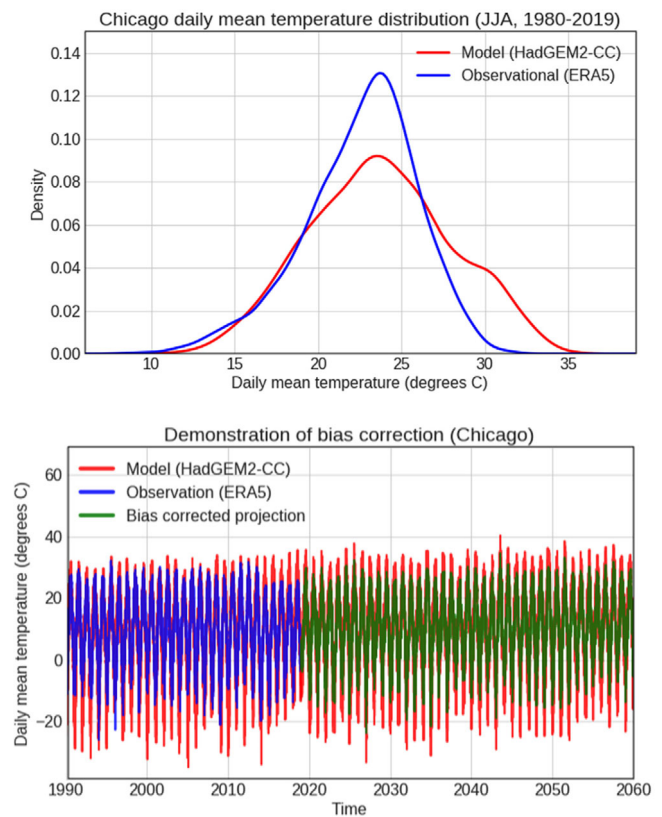


**FIGURE 1** Demonstrating the bias correction: comparison of summer (JJA) daily mean temperature distributions between raw model output (HadGEM2-CC) and ERA5 in Chicago (top); demonstration of bias correction as a timeseries of raw model output (HadGEM2-CC), observational data (ERA5) and bias-corrected output (bottom)

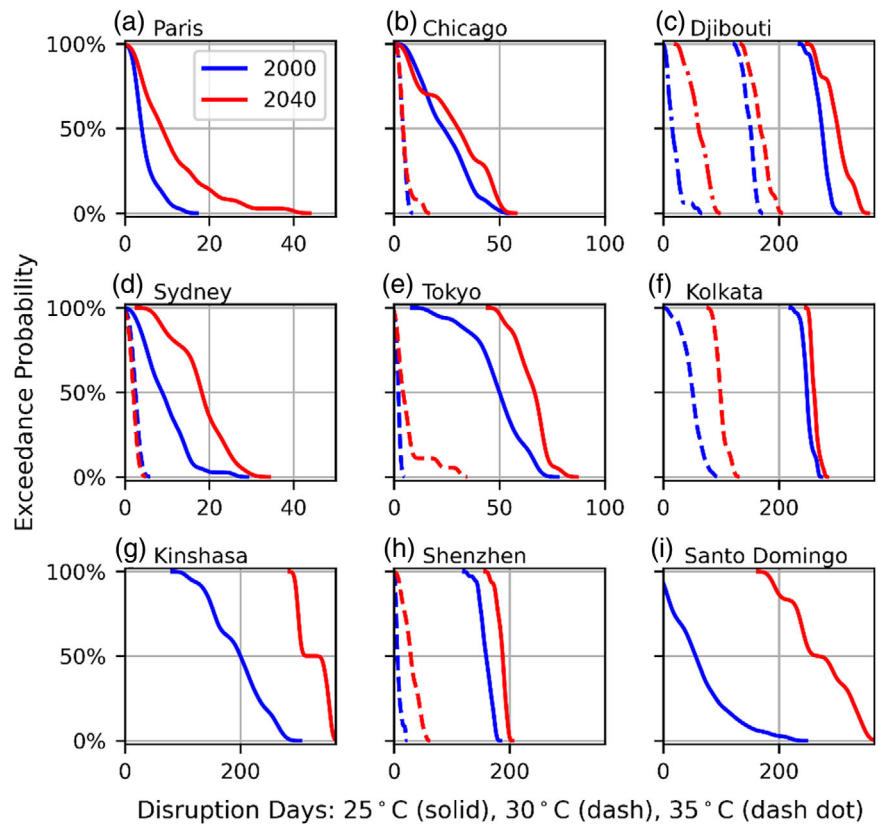
### 2.3 | Distribution of future temperature disruption days

The analysis of the bias-corrected data examines the 40-year period 2020–2059 and makes statistical predictions for the number of days with temperatures above a defined threshold in this period. This is what we refer to as the number of ‘disruption days’.

Counting the number of disruption days in each year during the period gives a distribution of 40 points. This can be visualized as an exceedance plot (i.e. 1 – CDF, the cumulative distribution function), showing, for a given probability, how many days are expected to be above a particular temperature. Given that the results have been analysed over a 40-year period, these results can be interpreted as the best estimate for a period centred on 2040, the midpoint of the analysis (although there is a long-term trend in temperatures over this period).

Given the relatively low granularity of the output (only 40 data points), kernel density estimation (KDE) is used to better visualize the underlying statistical process. The

**FIGURE 2** Exceedance plot of the number of disruption days above three mean daily temperature thresholds (25°C, 30°C and 35°C), for nine locations, from one model (HadGEM2-CC, red), compared with the historic measurements from ERA5 (blue)



KDE bandwidth used is varied for each location and temperature and corresponds to 6.7% of the 90%–10% days: Best practice for a Gaussian distribution would be approximately 15% (Silverman, B.W., 1986), but the authors feel that the long tails in this distribution justify a tighter bandwidth.

### 3 | RESULTS

#### 3.1 | Interpretation of a single location

Figure 2 shows outputs for a single model (HadGEM2-CC, red line, centred on 2040) for nine example locations from our global analysis, with up to three temperature thresholds (25°C, 30°C and 35°C), and compared with the ERA5 historic measurements (blue line, centred on 2000). The nearest city locations to the actual analysed points are given in Table 1. These nine example locations were chosen in order to represent a broad geographic spread of locations across all continents (excluding Antarctica).

The disruption days metric is based on specified mean daily temperature thresholds (25°C, 30°C and 35°C in this case), and the probability of a threshold being exceeded in any given year. This is shown on the vertical axes in Figure 2: for example, 10% exceedance probability corresponds to a once-per-decade event, or 1% corresponds to a

**TABLE 1** Nearest cities and the exact locations used in the analysis

| Nearest city  | Country   | Latitude, longitude |
|---------------|-----------|---------------------|
| Paris         | France    | 48.5 N, 2.5 E       |
| Chicago       | USA       | 41.5 N, 87.5 W      |
| Djibouti      | Djibouti  | 11.5 N, 42.5 E      |
| Sydney        | Australia | 33.4 S, 151.25 E    |
| Tokyo         | Japan     | 35.5 N, 139.5 E     |
| Kolkata       | India     | 22.5 N, 88.5 E      |
| Kinshasa      | D R Congo | 4.5 S, 15.5 E       |
| Shenzhen      | P R China | 22.74 N, 114.42 E   |
| Santo Domingo | Ecuador   | 0.5 S, 79.5 W       |

once-per-century event. These thresholds and exceedance probabilities can be adapted according to the business assets in question, to match with the acceptable level of risk to the asset operator or to reflect the relevant regional context.

Figure 2 illustrates that the modelled future changes in the number of disruption days vary widely by geographic location. For example, looking at the example of Paris in Figure 2(a), we see an increase of between 10 and 20 disruption days at the 25°C threshold (solid line), for low exceedance probabilities (i.e. 1-in-100- or 1-in-10-year

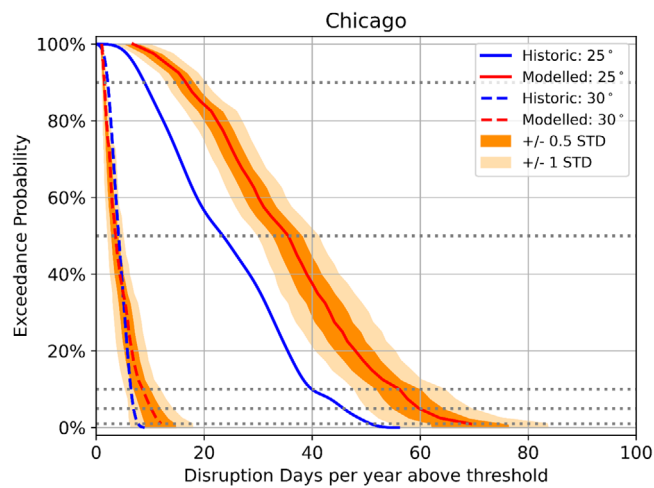


**FIGURE 3** Exceedance plot of the number of disruption days above two mean daily temperature thresholds, for one location, with example exceedance probabilities of 1%, 5%, 10%, 50% and 90% (grey dotted lines). The ensemble results from all 18 bias-corrected models are combined to give statistical measures

events), but only a small increase of just a few disruption days at higher exceedance probabilities. In contrast, for Santo Domingo in Ecuador (Figure 2i), we see a large increase of over 100 disruption days for the 25°C threshold at all exceedance probabilities. Kinshasa in DR Congo (Figure 2g) shows similarly large increases in the number of disruption days at the 25°C threshold. The other locations in Figure 2 also show increases in the number of disruption days at the 30°C threshold (dashed line), and for some (e.g. Kolkata, Figure 2f), the modelled increase at the 30°C threshold is greater than at the 25°C threshold. For Djibouti (Figure 2c), we see the greatest increase in the number of disruption days at the 35°C threshold (dashed-dotted line). Recall that these thresholds illustrate the mean daily temperature, and the peak daily temperature will be significantly higher.

### 3.2 | Combining results from all models

Each of the 18 models used provides a set of results for each of the approximately 18,000 locations. We combine the output from the ensemble of all models to give distributions over the models at each exceedance probability for each temperature threshold. The ensemble-mean provides a ‘best-guess’ estimate of the number of disruption days at a particular exceedance probability, while adding a number of standard deviations from the mean provides an indication of a worst case with a known degree of confidence. Figure 3 shows an example for a single location, the grid cell containing Chicago. The distribution of results between models allows us to give a measure of the assessed

likely range ( $\pm S$  std) of the prediction around model risk. Statements can be made in the format: ‘At location L, in the period centred on 2040, it is expected that one in N years will have D days disruption at a mean daily temperature above T, with S std of confidence’.

For example, referring to the results for Chicago given in Figure 3, we might be interested in a 1-in-10-year scenario, i.e., an exceedance probability, shown on the vertical axis, of 10%. The measurements show that historically there have been approximately 40 days per year, shown on the horizontal axis, where the mean daily temperature has exceeded 25°C (solid blue line): But with the impact of climate change, this is expected to rise to approximately 55 days (solid red line). Therefore, we can say: ‘In Chicago for the period centred on 2040, we expect every decade there will be one year where 55 days have a mean daily temperature above 25°C, up from 40 days for the period centred on 2000.’ The uncertainty between different models can be accounted for by the addition of the following statement: ‘there is a 16% chance that every decade one year will have 64 days exceeding this threshold’ (corresponding to +1 std). This is essential for planning worst-case scenarios and takes account of model risk by incorporating an ensemble of results from different groups.

Although the change in absolute number of days may be quite small (55 disruption days rather than 40), in a location which is historically ill-prepared for high temperatures, each day can cause a significant cost and an increase in the fraction of days lost could be very significant. One example might be locations in temperate regions that generally do not have air conditioning, where the investment needed to install widespread building cooling capacity would be very significant.

Another interpretation is to find the change in frequency for a given number of disruption days. Referring again to Figure 3, there is approximately 10% probability (i.e. 1-in-10-year expectation) of 40 disruption days with a mean daily temperature above 25°C at the baseline 2000 condition. Under climate change, for the period centred on 2040 the same number of disruption days is expected with about 38% likelihood, approximately 4-in-10 years. Thus, we can expect approximately four times the number of years with this number of disruption days.

This is often a more impactful way to understand the predictions. Risk and operation managers and senior executives might be tempted to regard a 1-in-10-year expected loss as simply a ‘risk of doing business’ which will generally be smoothed over with preceding and following ‘normal’ years. If, however, this loss approaches a 1-in-2 frequency, it will need to be addressed, mitigated or provisioned. We believe that this method of presenting the impacts of climate change is likely to promote meaningful change from operators and owners of economic assets.

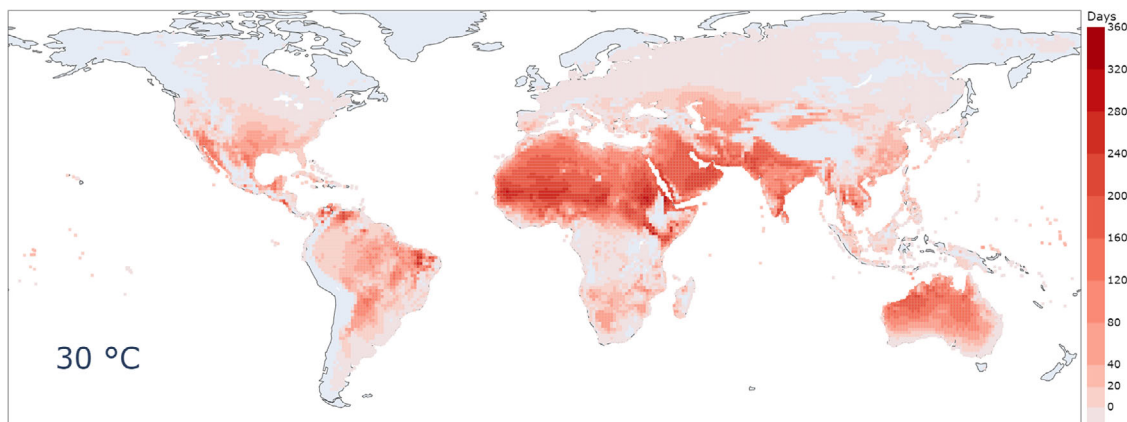


**FIGURE 4** Absolute number of daily mean disruption days per year over the 30°C temperature threshold for the 2020–2059 period, at a 1-year-in-10 exceedance probability

### 3.3 | Global depiction of results

The examples above demonstrate the presented methodology for individual cities, with a moderate temperature threshold. However, this technique is intended for a global application to enable risk analysis of the exposures of global activities and value chains: The example of Chicago above is also applicable to any global location. It is acknowledged that the use of an absolute temperature threshold (e.g. 30°C) has been criticized for not taking into account climate variability (Zuo et al., 2015). However, we suggest that the application of critical thresholds of disruption in this way is a useful method to assess global exposures in a systematic way. Differences in the coping capacity of a specific region or locale to extreme heat can be accounted for through variation of the vulnerability component of a risk calculation.

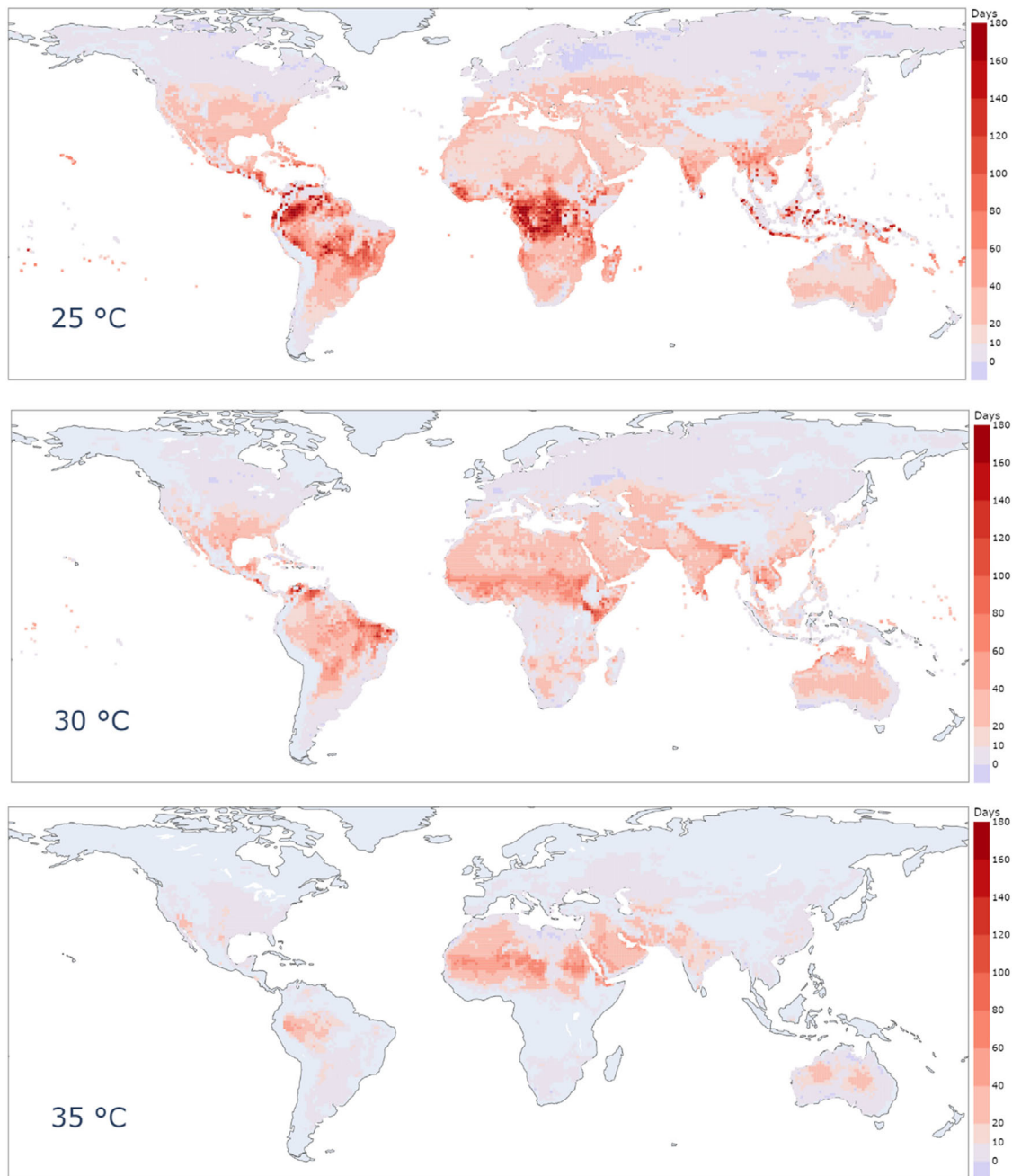
Figure 4 shows a global map of the absolute number of disruption days over the 30°C threshold for the 2020–2059 period, at a 10% exceedance probability (one year in 10). For each global location, the mean exceedance from all 18 of the bias-corrected models is used. It is clear from the map that for large parts of Saharan Africa, the Middle East and India, in the period centred on 2040, it is expected that 1-in-10 years will have at least 200 disruption days per year over the 30°C threshold, with some regions experiencing up to 360 disruption days per year. A large number of disruption days is also expected in Australia. Some parts of South America, in particular in the Amazon Basin, also show a large number of disruption days. In other regions, including Europe, sub-Saharan Africa and North America, the absolute number of expected disruption days per year at the 30°C threshold tends to be lower. However, while the absolute number of disruption days may seem low in some regions, the *increase* in the number of disruption days per year may still be higher. This is discussed below.

Figure 5 shows global maps of the expected increase in the number of disruption days from 1979–2018 to 2020–2059, using the threshold of mean daily temperature exceeding 25°C, 30°C and 35°C, with a 10% probability of exceedance (i.e. one year each decade). Differences in the impact between regions expected as a result of climate change can easily be seen. For example, Central America and sub-Saharan Africa have a high increase in daily mean 25°C disruption days, but the greatest impact at 35°C is in Saharan Africa and the Middle East, which likely are close to exceeding lower temperature thresholds for most days at historic conditions (illustrated for the example of Djibouti in Figure 2c). This distinction is important, as a temperature threshold that is impactful in one region of the world may be less relevant in another, demonstrating the need for regionally specific thresholds.

Maps such as these can be generated for any temperature or probability threshold, incorporating if necessary a measure to account for uncertainty between the climate models, by including a number of standard deviations from the mean between models at each location, as illustrated for a single location (Chicago) in Figure 3. This approach can be readily applied to risk assessment in a variety of domains, through analysis of the extreme heat hazard against exposures and vulnerabilities of specific sectors, such as agriculture (where agricultural risk models are used to calculate production disruption) or manufacturing (e.g. to assess rates of absenteeism/presenteeism, reduction of output, energy demands and air conditioning loads etc.).

### 3.4 | Aggregated global results

Although the primary focus of this paper is on providing localized estimations of the change in disruption days, it is also interesting to get a broad measure of the global change



**FIGURE 5** Expected increase in the number of daily mean 25°C (top), 30°C (middle) and 35°C (bottom) disruption days from 1979–2018 to 2020–2059, at a 1-year-in-10 exceedance probability, mean from all 18 bias-corrected models

in disruption days. To do so, we divide the globe into three zones by latitude: 0° to 23.5° ('tropical'), 23.5° to 35.5° ('sub-tropical') and 35.5° to 70° ('temperate'). For each landmass grid square in each zone and at each temperature threshold, we calculate the mean of the baseline number of disruption days and the mean of the increase in disruption days expected from 1979–2018 to 2020–2059. The results are shown in Table 2.

This averaged analysis, of course, hides a large amount of local data: Some localities will have a much larger increase in the number of disruption days and some may

have no increase or even a slight decrease (for example some regions of Russia and Canada show a decrease in Figure 5).

Given the wide distribution in the increase in the number of disruption days, a more informative way to analyse the data is to ask what fraction of locations in each zone have more than a given number of days increase. We show this fraction in Table 3 for the same temperature thresholds and latitude zones, for 10 and 30 days.

Tropical regions are impacted the most with highest fraction of locations suffering 30 additional days. For



**TABLE 2** Mean number of disruption days, and mean increase, for three latitude zones at three temperature thresholds

| Threshold temp (daily mean) | Zone        | Mean baseline number of disruption days for 1979–2018 | Mean increase in number of disruption days from 1979–2018 to 2020–2059 |
|-----------------------------|-------------|---|--|
| 25°C                        | Tropical    | 237   | 39   |
|                             | Subtropical | 125   | 20   |
|                             | Temperate   | 16  | 8  |
| 30°C                        | Tropical    | 51  | 26   |
|                             | Subtropical | 56  | 20   |
|                             | Temperate   | 5   | 6  |
| 35°C                        | Tropical    | 17  | 19   |
|                             | Subtropical | 19  | 12   |
|                             | Temperate   | 1.3   | 4.2  |

**TABLE 3** Fractional increase in the number of locations predicted to have 10 and 30 additional disruption days, for three latitude zones at three temperature thresholds

| Threshold temp (daily mean) | Zone        | Fraction of locations with more than 10 disruption days increase | Fraction of locations with more than 30 disruption days increase |
|-----------------------------|-------------|--|--|
| 25°C                        | Tropical    | 77%  | 44%  |
|                             | Subtropical | 82%  | 12%  |
|                             | Temperate   | 20%  | 1%   |
| 30°C                        | Tropical    | 64%  | 28%  |
|                             | Subtropical | 66%  | 16%  |
|                             | Temperate   | 7%   | 0%   |
| 35°C                        | Tropical    | 24%  | 12%  |
|                             | Subtropical | 29%  | 7%   |
|                             | Temperate   | 1%   | 0%   |

10 days, subtropical regions are approximately equally affected, with temperate latitudes the least impacted. It is worth remembering though that temperate regions may have the biggest financial sensitivity to the disruption days, since many locations will be relatively poorly prepared.

## 4 | DISCUSSION

Although in some cases the absolute increase in the number of disruption days in the results discussed above is relatively small, we must remember that:

- This analysis is performed on daily mean temperatures, so a daily peak temperature will be significantly higher
- Economic processes slow down very rapidly with rising temperature, so (for instance) the prospect of a threefold increase in the number of economically unproductive days would be highly impactful
- The strong variation between locations (illustrated in Figures 2 and 5) shows that this mean increase includes many locations with a much higher increase
- Some locations will be less prepared than others. For example, housing and workspaces in many temperate locations do not have air cooling. As a result, an increase in the number of days at even a low temperature threshold could have a higher economic impact than at a subtropical location, where at least there is a higher level of preparedness to hot days.

### 4.1 | Localized economic impacts

Extreme climate events are known to cause devastating damage, both in human lives and in financial assets. The future ‘climate value at risk’ of global financial assets is US\$2.5 trillion in the ‘business-as-usual’ scenario, while the 99th percentile of the possible outcomes gives the value of approximately US\$24.2 trillion (Dietz et al., 2016). In addition, climate–economic models show that losses from climate change may reach 23% of the global gross product by the end of 2100 (Burke et al., 2015; Patrycja et al., 2021). Since 1970, estimates show that weather-related natural disasters alone caused losses of around US\$1.2 trillion and claimed approximately 1.6 million lives (Swiss Re, 2021).

Heatwaves have shown increasing trends in frequency, duration and cumulative heat since the mid-20th century, and have also shown signs of acceleration of those trends in the presence of global warming (Perkins-Kirkpatrick & Lewis, 2020). Those upward trends can be seen in the recent past of such events – the major European heatwaves of 2003 and 2019 were just 16 years apart but were estimated to be 1-in-450-year and 1-in-283-year events, respectively (Ma et al., 2020; Munich Re, 2004). Those types of events can be catastrophic for people, countries and businesses, especially if mitigation plans are not in place. The 2003 European heatwave claimed an estimated 35,000 lives, 14,947 out of those in France alone, a country without a strategy against heatwaves at the time (Larsen, 2003; Poumadere et al., 2006). Estimates of the financial cost for this event alone are around US\$13 billion, mostly in agricultural costs, which is believed to be a conservative estimate as crops were not usually insured in Europe in 2003 (de Bono et al., 2004; Munich Re, 2004).

Providing economic loss calculations due to future heatwaves is outside the scope of this paper, but the methods

and results showcased in this study can provide a good baseline for such estimations. For example, making an assumption that the 1995 Chicago heatwave was a 1-in-100-year event (Karl & Knight, 1997) and the fact that this event is part of the 1979–2018 timeseries, one can use our disruption days framework to estimate the probability of a similar event arising in the 2040-centred period. Reading from Figure 3, in terms of the same number of disruption days (both 25°C and 30°C thresholds), the probability of having a similar event would increase to 10% (or 1-in-10 years). This result is limited not only by the aforementioned assumption, but also by the assumption that the ‘disruption days per year’ metric is perfectly correlated with the emergence of heatwaves. The lack of higher precision in distributions of this metric can also have an effect on this result as the smallest increment in our exceedance probability plots is 2.5%, while the event is assumed to have a probability of 1%. However, this result shows the potential of this type of analysis for the mitigation of future extreme weather events.

By knowing the sensitivity to temperatures and the geographic distribution of their operations, it would be feasible for an organization to quantify their expected total financial loss due to temperature disruption days. This could be essential for provisioning, insurance or risk reporting, including TCFD disclosures. It also lays the foundations for planning strategic responses to physical climate change risk.

Finally, we must remember that the global economy can be highly concentrated on small regions. In an economic ecosystem with small amounts of ‘slack’ in supply chains, a minor disruption to one part can be highly magnified in its overall impact. In this context, even a relatively small change in the number of disruption days at a systemically important location could impact well beyond the affected area. One example of these is logistics hubs: A major disruption at an international port could have long-term, global impacts. This consequence of fragile supply chains underlines further the importance of matching the research described here with a comprehensive economic model.

## 5 | FUTURE WORK

The procedures described in this paper give the first stage of assessing a financial cost at a relatively local resolution from extreme temperature effects, expressed as ‘disruption days’. However, it needs to be followed by assessments at a local level of economic vulnerability to disruption days. These could be as simple as ‘the airport will close if the mean daily temperature is above 35°C’ or ‘the cost of electricity generation for the region rises by US\$50 mil-

lion for each day above 30°C’. At the other extreme, a complex, multi-location operation could assess operations at each location, and apply these vulnerabilities to the disruption days calculated here to give a total expected additional cost. By combining all significant economic activity in a region and estimating vulnerability to extreme weather, it would be possible for a local or national government to estimate the gross effect of temperature disruption days on their economy. A multinational company with economically productive assets spread over many locations could do the same.

The general approach used in this study (re-gridding at relatively fine spatial granularity, bias correction of individual models, calculation of the disruption days for each model at each location, followed by ensemble averaging over models to get model risk statistics) can equally well be applied to other extreme weather features which are likely to be affected by climate change, and could be the subject of future work:

- Precipitation. Droughts and flooding have profound effects on many natural and human activities, not least agriculture
- Multivariate analysis of compound risks. For example, the impacts of humidity combined with temperature, or drought combined with high temperature
- Low temperature thresholds. Frost days, for example, can limit economic activity in some temperate regions, where freezing temperatures are relatively rare and preparedness is low
- Quantifying maximum or minimum daily temperatures, rather than mean daily temperatures, might also be interesting as many activities are more accurately limited by daily extremes rather than mean temperatures.

The methodological analysis presented in this paper could be improved in future studies as and when new datasets and methods become available. In terms of data preparation and pre-analysis, machine learning methods show great promise in improving existing bias correction techniques, and such new methods could be applied to repeat and improve our analysis presented here. While this study has focussed on the use of model results from the CMIP5 generation of climate models, the newly available generation of CMIP6 models have a higher spatial resolution and would allow for the approach in this paper to be repeated with finer geographic grids.

## 6 | CONCLUSION

Using multi-model, bias-corrected results from CMIP5 climate models, we estimate the frequency of daily mean

temperatures exceeding certain temperature thresholds on ‘disruption days’, at given locations for a future period centred on 2040, compared with historical observations from ERA5 centred on 2000. Since it is often the exceedance over a threshold, rather than simply the mean annual temperature, that is the determining factor for economic activity, this approach is expected to be a better indicator on the effect of climate change on human and economic activity.

Our results allow for the estimation of the increase in the number of disruption days exceeding a certain temperature threshold for a given location and exceedance probability. For example, in Chicago one can expect that by 2040, every decade there will be one year where 55 days have a mean daily temperature above 25°C, up from 40 days for the period centred on 2000. Another way to read the results is that Chicago can expect a fourfold increase in the number of years with at least 40 disruption days above the 25°C threshold by 2040.

Globally, our results also show that there is broad variation in the modelled increase in number of disruption days, for different locations, temperature thresholds and exceedance probabilities. Central America and sub-Saharan Africa show the largest increases in number of disruption days at the 25°C temperature threshold, while the greatest increases in disruption days exceeding 35°C are seen in Saharan Africa and the Middle East.

By combining these results with the sensitivities of economic activities to temperature thresholds (not described in this paper), it will become possible to estimate the financial impact of climate change on a wide variety of businesses. Examples are logistics (frequently disrupted by weather extremes), outdoor work (where human productivity rapidly falls with temperature) and agricultural yields (which typically fall once a crop-dependent temperature threshold is passed).

By knowing locations and the nature of activities through an organization, it will be possible to estimate, with a given level of confidence over model risk, the financial impact of climate change-related changes in temperature.

## REPRODUCIBLE MATERIAL FROM OTHER SOURCES

Except where noted, material from other sources has not been used.

## ACKNOWLEDGEMENT

The authors would like to express gratitude to Professor Daniel Ralph and Mr Oliver Carpenter at The Centre for Risk Studies, University of Cambridge, Judge Business School.

## CONFLICTS OF INTEREST

The authors are unaware of any conflicts.

## FUNDING

No directed funding was used for this work.

## ORCID

Tim Summers  <https://orcid.org/0000-0001-5955-150X>

## REFERENCES

- Bono, A., Giuliani, G., Kluser, S. & Peduzzi, P. (2004) Impacts of summer 2003 heat wave in Europe. *UNEP/DEWA/GRID Europe. Environment Alert Bulletin*, 2 (January), 1–4.
- Burke, M., Hsiang, S.M. & Miguel, E. (2015) Global non-linear effect of temperature on economic production. *Nature*, 527(7577), 235–239. <https://doi.org/10.1038/nature15725>
- Ciavarella, A., Cotterill, D., Stott, P., Kew, S., Philip, S., Jan van Oldenborgh, G., et al. (2021) Prolonged Siberian heat of 2020 almost impossible without human influence. *Climatic Change*, 166(1), 9. <https://doi.org/10.1007/s10584-021-03052-w>
- Dietz, S., Bowen, A., Dixon, C. & Gradwell, P. (2016) “Climate value at risk” of global financial assets. *Nature Climate Change*, 6(7), 676–79.
- Eccles, R. & Krzus, M. (2018) Why companies should report financial risks from climate change. *MIT Sloan Management Review*, 59, 1–6.
- Forzieri, G., Bianchi, A., Silva, F.B.e., Herrera, M.A.M., Leblois, A., Laval, C., et al. (2018) Escalating impacts of climate extremes on critical infrastructures in Europe. *Global Environmental Change*, 48(January), 97–107. <https://doi.org/10.1016/j.gloenvcha.2017.11.007>
- García-León, D., Casanueva, A., Standardi, G., Burgstall, A., Flouris, A.D. & Nybo, L. (2021) Current and projected regional economic impacts of heatwaves in Europe. *Nature Communications*, 12(1), 5807. <https://doi.org/10.1038/s41467-021-26050-z>
- Gudmundsson, L., Bjornar Bremnes, J., Haugen, J. & Skaugen, T. (2012) ‘Technical note: downscaling RCM precipitation to the station scale using quantile mapping – a comparison of methods. *Hydrology and Earth System Sciences Discussions*, 9(May), 6185–6201. <https://doi.org/10.5194/hessd-9-6185-2012>
- Haerter, J.O., Hagemann, S., Moseley, C. & Piani, C. (2011) Climate model bias correction and the role of timescales. *Hydrology and Earth System Sciences*, 15(3), 1065–1079. <https://doi.org/10.5194/hess-15-1065-2011>
- Handmer, J., Honda, Y., Kundzewicz, Z.W., Arnell, N., Benito, G., Hatfield, J., et al. (2012) Changes in impacts of climate extremes: human systems and ecosystems. In: Field, C.B., Barros, V., Stocker, T.F. & Dahe, Q. (Eds.) *Managing the risks of extreme events and disasters to advance climate change adaptation*. Cambridge: Cambridge University Press, pp. 231–290. <https://doi.org/10.1017/CBO9781139177245.007>
- Hawkins, E., Osborne, T.M., Ho, C.K. & Challinor, A.J. (2013) Calibration and bias correction of climate projections for crop modelling: an idealised case study over Europe. *Agricultural and Forest Meteorology*, 170, 19–31. <https://doi.org/10.1016/j.agrformet.2012.04.007>
- Hempel, S., Frieler, K., Warszawski, L., Schewe, J. & Piontek, F. (2013) A trend-preserving bias correction – the ISI-MIP approach. *Earth System Dynamics Discussions*, 4, 49–92. <https://doi.org/10.5194/esdd-4-49-2013>

- Hersbach, H., Bell, B., Berrisford, P., Hirahara, S., Horányi, A., Muñoz-Sabater, J., et al. (2020) The ERA5 global reanalysis. *Quarterly Journal of the Royal Meteorological Society*, 146(730), 1999–2049. <https://doi.org/10.1002/qj.3803>
- IPCC. (2021) Summary for policymakers. In: Climate change 2021: the physical science basis. Contribution of Working Group I to the Sixth Assessment Report of the Intergovernmental Panel on Climate Change. 2021. <https://www.ipcc.ch/report/ar6/wg1/>
- Karl, T.R. & Knight, R.W. (1997) The 1995 Chicago heat wave: how likely is a recurrence? *Bulletin of the American Meteorological Society*, 78(6), 1107–1120. [https://doi.org/10.1175/1520-0477\(1997\)078<1107:TCHWHL>2.0.CO;2](https://doi.org/10.1175/1520-0477(1997)078<1107:TCHWHL>2.0.CO;2)
- Larsen, J. (2003) Plan B updates – 29: Record heat wave in Europe takes 35,000 lives – far greater losses may lie ahead | EPI. 2003. [http://www.earth-policy.org/plan\\_b\\_updates/2003/update29](http://www.earth-policy.org/plan_b_updates/2003/update29)
- Ma, F., Yuan, X., Jiao, Y. & Ji, P. (2020) Unprecedented Europe heat in June–July 2019: risk in the historical and future context. *Geophysical Research Letters*, 47(11), E2020GL087809. <https://doi.org/10.1029/2020GL087809>
- Maraun, D. (2013) Bias correction, quantile mapping, and downscaling: revisiting the inflation issue. *Journal of Climate*, 26(6), 2137–2143. <https://doi.org/10.1175/JCLI-D-12-00821.1>
- Maraun, D., Shepherd, T.G., Widmann, M., Zappa, G., Walton, D., Gutiérrez, J.M. et al. (2017) Towards process-informed bias correction of climate change simulations. *Nature Climate Change*, 7(11), 764–773. <https://doi.org/10.1038/nclimate3418>
- Maraun, D. & Widmann, M. (2018) *Statistical downscaling and bias correction for climate research*. Cambridge: Cambridge University Press. <https://doi.org/10.1017/9781107588783>
- Mora, C., Dousset, B., Caldwell, I.R., Powell, F.E., Geronimo, R.C., Bielecki, C.R. et al. (2017) Global risk of deadly heat. *Nature Climate Change*, 7(7), 501–506. <https://doi.org/10.1038/nclimate3322>
- Munich Re. (2004) TOPICS Geo 2003. *TOPICS Geo*, 2003. [http://www.sfu.ca/geog312/readings/Munich%20Re\(2004\).pdf](http://www.sfu.ca/geog312/readings/Munich%20Re(2004).pdf)
- Oldenborgh, G.J., Krikken, F., Lewis, S., Leach, N.J., Lehner, F., Saunders, K.R. et al. (2020) Attribution of the Australian bushfire risk to anthropogenic climate change. *Natural Hazards and Earth System Sciences Discussions*, 21, 941–960. <https://doi.org/10.5194/nhess-2020-69>
- Patrycja, K., Agarwala, M., Burke, M., Kraemer, M. & Mohaddes, K. (2021) Rising temperatures, falling ratings: the effect of climate change on sovereign creditworthiness. 2021. Working paper. The Bennett Institute for Public Policy. <https://www.bennettinstitute.cam.ac.uk/publications/rising-temperatures-falling-ratings/>
- Perkins-Kirkpatrick, S.E. & Lewis, S.C. (2020) Increasing trends in regional heatwaves. *Nature Communications*, 11(1), 3357. <https://doi.org/10.1038/s41467-020-16970-7>
- Poumadere, M., Mays, C., Mer, S. & Blong, R. (2006) The 2003 heat wave in France: dangerous climate change here and now. *Risk Analysis*, 25(January), 1483–1894. <https://doi.org/10.1111/j.1539-6924.2005.00694.x>
- Quarles, R.K. (2021) Status report: task force on climate-related financial disclosures. [https://assets.bbhub.io/company/sites/60/2021/07/2021-TCFD-Status\\_Report.pdf](https://assets.bbhub.io/company/sites/60/2021/07/2021-TCFD-Status_Report.pdf)
- Seneviratne, S.I., Zhang, X., Adnan, M., Badi, W., Dereczynski, C., Luca, A.D. et al. (2021) Weather and climate extreme events in a changing climate. In: Masson-Delmotte, V., Zhai, P., Pirani, A., Connors, S.L., Péan, C., Berger, S. et al. (Eds.) *Climate change 2021: the physical science basis. Contribution of working group I to the sixth assessment report of the intergovernmental panel on climate change*. Cambridge: Cambridge University Press.
- Silverman, B.W. (1986) *Density estimation for statistics and data analysis*. London: Chapman & Hall/CRC.
- Simpson, C., Hosking, J.S., Mitchell, D., Betts, R.A. & Shuckburgh, E. (2021) Regional disparities and seasonal differences in climate risk to rice labour. *Environmental Research Letters*, 16(12), 124004. <https://doi.org/10.1088/1748-9326/ac3288>
- Re, S. (2021) Sigma explorer. *Sigma Explorer*. <https://www.sigmaexplorer.com>
- TCFD. (2020) Recommendations. *Task Force on Climate-Related Financial Disclosures (blog)*. <https://www.fsb-tcfd.org/recommendations/>
- Xia, Y., Li, Y., Guan, D., Mendoza Tinoco, D., Xia, J., Yan, Z., et al. (2018) Assessment of the economic impacts of heat waves: a case study of Nanjing, China. *Journal of Cleaner Production*, 171, 811–819. <https://doi.org/10.1016/j.jclepro.2017.10.069>
- Zuo, J., Pullen, S., Palmer, J., Bennetts, H., Chileshe, N. & Ma, T. (2015) Impacts of heat waves and corresponding measures: a review. *Journal of Cleaner Production*, 92, 1–12. <https://doi.org/10.1016/j.jclepro.2014.12.078>

**How to cite this article:** Summers, T., Mackie, E., Ueno, R., Simpson, C., Hosking, J.S., Suci, T. et al. (2022) Localized impacts and economic implications from high temperature disruption days under climate change. *Climate Resilience and Sustainability*, 1, e35. <https://doi.org/10.1002/cli2.35>

## Appendix

The CMIP5 models used are ACCESS1-3, BNU-ESM, CMCC-CMS, CNRM-CM5, CSIRO-Mk3-6, GFDL-CM3, GFDL-ESM2G, GFDL-ESM2M, HadGEM2-CC, HadGEM2-ES, IPSL-CM5A-LR, IPSL-CM5A-MR, IPSL-CM5B-LR, MPI-ESM-LR, MPI-ESM\_MR, NorESM1-M, bcc-csm1-1 and inmcm4. A small number of other models were not included either because they had been superseded by later models from the same research group or because of data incompatibilities.